23rd ABCM International Congress of Mechanical Engineering
December 6-11, 2015, Rio de Janeiro, RJ, Brazil

Non-stationary Gaussian Process as a surrogate for modelling hydraulic fracture in a multilayer rocky medium

Souleymane Zio
Fernando Alves Rochinha
mechanical engineering - Federal University of Rio de Janeiro (UFRJ)
zio@ufrj.br

Abstract. *Complex computer models are widely used to predict the behavior of complex physical phenomena. However, these computer models become too expensive when taking into account variability present in the physical properties. To circumvent this problem, the expensive computer model is replaced by the inexpensive mathematical function, called surrogates. In this work, we use the nonstationary multivariate Gaussian process (MGPs) as the surrogate to predict the evolution of hydraulic fracture(HF) in the rocky medium which present 3 layers separated by 2 interfaces. The mathematical model of the HF relies on complex non-linear and free boundary problems simulated here, through an implicit level set algorithm. The numerical examples are presented to show the efficiency of the MGPs to predict the evolution of the HF in the rock which presents discontinuities and uncertainty in the rock properties. The MGPs results are compared to the Monte Carlo method(MC) and the stochastic collocation method (SCM).*
Keywords: *Nonstationary, Gaussian Process, Hydraulic Fracture , Uncertainty*

1. INTRODUCTION

Hydraulic fracturing is a process used in the oil and gas industry to improve the permeability of the rock. This process usually occurs in reservoirs that have heterogeneity and complexity in the description of the properties that are not well known (shale gas). This may be due to the limited number of experiments used to obtain information about the properties of the reservoir. It may also be due to the complexity of rocks that may have natural fractures, layers of different properties and heterogeneous confining stress. However to obtain a reliable and robust hydraulic fracturing solution, the numerical simulation must account for uncertainties about the properties of rocks. The HF computer code is too time expensive to propagate the uncertainty using the sampling method such as the Monte Carlo method (MC). In this case, to avoid this problem, the complex computer code is replaced by the mathematical approximation called surrogate (George Shu Heng Pau, 9 May 2013). The literature presents several surrogates built using the Gaussian Process, Polynomial function, and neutral networks. Here due to the non-smooth behavior of HF evolving in the multiple layers rocky, We construct the surrogate using the non-stationary Multivariate Gaussian process (MGPs) which can be ideal to approximate the non-smooth HF response Gibbs (1997). Herein, the non-stationary MGPs are obtained by dividing adaptively the input space into disjoint subspace and at each subspace we use the MGPs to calculate the predictive statistic. The criterion to divide the input space in subspace depends on the variance or the error bar provided by the Gaussian process approximation. If the error bar is greater than the desired value, the input space is divided into two subspaces and the process is applied at each new subspace. At the end of the process, all subspace must have the error bar less than the desired value.

The multivariate GP is obtained by considering that all the outputs are independent and have the same covariance function at each subspace. The global predictive statistics are obtained by the combination of the statistics obtained at each subspace.

The multivariate GP is obtained by considering that all the outputs are independent and have the same covariance function at each subspace. The global predictive statistics are obtained by the combination of the statistics obtained at each subspace. The efficiency of the MGP to approximate the HF fracture in rocky presenting 3 layers and 2 interfaces is compared to the sampling method such as Monte Carlo and to the Stochastic collocation method (Ma and Zabaras, 2008). In the next section, we present the modelling of the HF evolution which can be approximated using the implicit level set algorithm proposed by (Peirce and Detourney, 2008). In section 2 we present the methodologies to construct the MGP following the (Ilias Bilionis, 2013) approach. In section 3 we present the numerical results and the conclusion in the last section.

2. Hydraulic fracture modeling

Assuming a plane strain state, the elastic problem, and consequently the flow problem, is reduced to a one-dimensional spatial setting (Peirce, Received 2 May 2014 accepted 22 August 2014 Available online 28 September 2014) with coordinate x coincident with the fracture propagation direction and occupying a domain that evolves with the time t described by the interval $\ell(t) = [l_{low}(t), l_{up}(t)]$. The fracture is propagated by the injection, through the well, of an incompressible Newtonian fluid with dynamic viscosity μ. As the flow takes place in the confined interior volume of the fracture delimited by its aperture $w(x,t)$, lubrication equation is assumed to model the flow behavior characterized by the pressure $p_f(x,t)$ and fluid flux $q(x,t)$. The whole process is controlled by the injection rate Q_0 and the physical and geological conditions imposed by the rock formation, namely: the confining stress σ, perpendicular to the fracture aperture direction, and the four material parameters E', μ', K', and C' defined as: $E' = \frac{E}{1-\nu^2}$; $\mu' = 12\mu$; $K' = 4(\frac{2}{\pi})^{\frac{1}{2}} K_{ic}$; $C' = 2C_l$. Here, E' is the plane strain modulus, μ' the alternate viscosity, C' the leak-off coefficient and K' the rock toughness.

The governing equations are presented below in a dimensionless form resulting from a scaling the allows to unveil the different fracture evolution regimes, which will not be discussed here due to the lack of space, but are pivotal in the design of the numerical approach proposed in (Peirce and Detourney, 2008). This scaling introduces characteristics length, time, pressure, and fracture opening: ℓ_*, t_*, w_*, p_*, to be determined in line with the aforementioned propagation regimes. Therefore, the quantities of interested are expressed as: $x = \ell_* \chi$,$t = t_* \tau$, $w = w_* \Omega$, $p_f = p_* \Pi_f$, $\sigma_0 = p_* \Sigma_0 \Phi(\chi)$, $Q = Q_0 \Psi(\tau)$. The quantities $\chi, \tau, \Omega, \Pi_f$ represent the dimensionless spatial coordinate, time, fracture aperture and fluid pressure. Moreover, $\Phi(\chi)$ is the spatial distribution of the confining stress.

Elasticity Equation

$$\Pi = \Pi_f(\chi,\tau,\varpi) - \Sigma_0(\varpi)\Phi(\chi,\varpi) = \frac{-G_E}{4\pi} \int_{-\ell_{low}(\tau,\varpi)}^{\ell_{up}(\tau,\varpi)} \frac{\Omega(\chi',\tau,\varpi)}{(\chi-\chi')} d\chi', \tag{1}$$

where $\Pi(\chi,\tau,\varpi)$ stands for the nondimensional net pressure (resulting from the difference between fluid pressure and the geological confining stresses).

Lubrication Equation:

$$\frac{\partial \Omega}{\partial \tau} + G_c \frac{H(\tau - \tau 0(\chi))}{\sqrt{(\tau - \tau_0(\chi))}} = G_m \frac{\partial}{\partial \chi}[\Omega^3 \frac{\partial \Pi_f}{\partial \chi}] + G_v \Psi \delta_0(\chi), \tag{2}$$

where H is the Heaviside function and δ_0 is the Dirac function centered at the injection points.

Boundary and Propagation Conditions:

$$\begin{aligned} &\lim_{\xi \to 0} \Omega^3 \frac{\partial \Pi_f}{\partial \xi} = 0, \\ &\Omega(\ell_{low,lup}, ., .) = 0, \end{aligned} \tag{3}$$

$$\lim_{\xi \to 0} \frac{\Omega}{\xi^{1/2}} = G_k, \tag{4}$$

where $\xi = \ell(\tau, .) - \chi$ is a local coordinate representing the distance from a fracture interior point to the fracture tip. The first condition corresponds to no flux through the tips; the second implies that the fracture aperture vanishes, and the third one reflects the aperture asymptotic behavior corresponding to the linear fracture mechanics. The dimensionless quantities G_j above, whose values determine the propagation regimes, are defined as follows: $G_E = \frac{p_* \ell_*}{E' w_*}$, $G_m = \frac{\mu' Q_0}{w_*^3 p_*}$, $G_v = \frac{Q_0 t_*}{w_* \ell_*^2}$, $G_c = \frac{C' \ell_*^2}{Q_0 t_*^{1/2}}$, $G_k = \frac{K' \ell_*^{1/2}}{E' w_*}$.

Locating the free boundary using the tip asymptotics

Admitting $G_E = G_m = G_v = O(1)$, the above equations correspond to the viscosity dominate propagation regime (Peirce and Detourney, 2008), in which the viscous flow is the main dissipation mechanism, the tip fracture (within the spatial scale introduced by the numerical method) follows the asymptotic trend

$$\lim_{\xi \to 0} \Omega \sim \beta_{m0} V^{1/3} \xi^{2/3}, \tag{5}$$

where $\beta_{m0} = 2^{1/3} 3^{3/6} (\frac{\mu'}{E'})$, and V the normal velocity of the front, what is explored in the numerical scheme proposed in Peirce and Detourney (2008).

Besides the space and time coordinates χ and τ, we introduce above ϖ, a third argument for the fields above, in order to represent the random dimension needed for describing uncertainties in the input parameters within a probabilistic perspective. Here, we follow the same approach presented in (Zio and Rochinha, 2012)

3. Nonstationary Multi-output Gaussian Process (MGPs)

In order to make the presentation simpler and more compact, we adopt a simplified in which the simulator, understood here as a mapping connecting inputs (material and control parameters, initial conditions,...) and outputs (variables or quantities of interest like, for instance, fracture length and aperture, velocity of propagation), is denoted as $\mathbf{f}(\mathbf{x})$ with a $\mathbf{K}$-dimensional input $\mathbf{x} \in \mathbf{X} \subset \mathbf{R^K}$, i.e. $\mathbf{X} = \times_{k=1}^{\mathbf{K}}[a_k, b_k]$, $-\infty \leq a_k < b_k \leq \infty$. The probability density $p(\mathbf{x})$ defined for all $\mathbf{x} \in \mathbf{X}$ such as:

$$p(\mathbf{x}) = \prod_{k=1}^{K} p_k(x_k), \tag{6}$$

where $p_k(x_k)$ is the probability density pertaining to the k-th dimension. The outputs of the simulator $\mathbf{y} \in \mathbf{Y} \subset \mathbf{R^M}$, where $\mathbf{M}$ represents the number of outputs. The simulator is run at training input $\mathbf{X} = (\mathbf{x}^1, ..., \mathbf{x}^N)$, giving the training outputs $\mathbf{Y} = (\mathbf{y}_r^1 = \mathbf{f}(\mathbf{x^1}), ..., \mathbf{y}_r^N = \mathbf{f}(\mathbf{x})^N)$ where $\mathbf{r} = \mathbf{1}, .., \mathbf{M}$. We assume that we have observed a fixed number $N \geq 1$ and training set $\mathbf{D} = \{(\mathbf{X}, \mathbf{Y})\}$. The training outputs $\mathbf{Y}$ are used to calculate the mean and standard deviation of the observation. The observed mean and variance are calculated as follows:
The observed mean is:

$$\mu_{\mathbf{obs,r}} = \frac{\mathbf{1}}{\mathbf{N}} \sum_{\mathbf{n=1}}^{\mathbf{N}} \mathbf{y_r^n}, \tag{7}$$

and the observed variance is:

$$\sigma^{\mathbf{2}}_{\mathbf{obs,r}} = \frac{\mathbf{1}}{\mathbf{N}} \sum_{\mathbf{n=1}}^{\mathbf{N}} (\mathbf{y_r^n} - \mu_{\mathbf{obs,r}})^{\mathbf{2}}, \tag{8}$$

the scaled version $\mathbf{z}_r$ of the observation is used to put all output in the same signal strength, defined by:

$$\mathbf{z_r^n} = \frac{\mathbf{y_r^n} - \mu_{\mathbf{obs,r}}}{\sigma_{\mathbf{obs,r}}}. \tag{9}$$

From a Bayesian perspective, we regard $\mathbf{f}(.)$ as an unknown function (S. Conti, 1992). We consider that the prior information about $\mathbf{f}(.)$ is a Gaussian Process GPs conditional on the hyper-parameters (Stefano Conti, 2010). The posterior distribution of $\mathbf{f}(.)$ is regarded as the surrogate is also Gaussian process conditional on the hyper-parameters.

$$\mathbf{f}(.) \sim \mathbf{GP}(\mathbf{m}(\mathbf{x}), \mathbf{C}(\mathbf{x}, \mathbf{x'}; \Theta)), \tag{10}$$

where $\mathbf{m}(\mathbf{x})$ and $\mathbf{C}(\mathbf{x}, \mathbf{x'}; \Theta)$ are the mean and the covariance function of the GPs and Θ the unknown hyper-parameters. The hyper-parameters Θ= $(\mathbf{s_f}, \ell_{\mathbf{1}}, ..., \ell_{\mathbf{k}})$ are obtained by maximizing the logarithm of the marginal likelihood. Here, we use the Conjugate Gradient method(CG) to maximize the log-likelihood. Considering that the scaled responses are conditionally independent given Θ, the marginal likelihood is simply the sum of the marginal likelihood of each output:

$$\begin{aligned}
\ell(\Theta) &= \log p(\mathbf{z}_1, .., \mathbf{z}_M|\Theta) \\
\ell(\Theta) &= -\frac{\mathbf{1}}{\mathbf{2}} \sum_{\mathbf{r=1}}^{\mathbf{M}} \mathbf{z_r^T C^{-1} z_r} - \frac{\mathbf{M}}{\mathbf{2}} \log |\mathbf{C}| - \frac{\mathbf{NM}}{\mathbf{2}} \log \mathbf{2}\pi,
\end{aligned}$$

where $\mathbf{C} = \mathbf{C}_{nm} = \mathbf{C}(\mathbf{x}_n, \mathbf{x'}_m; \Theta)$, $\{n, m\} = 1, .., N$, and $|\mathbf{C}|$ its determinant.
Thus Θ is obtained by maximize $\ell(\Theta)$:

$$\Theta^* = \arg\max_{\Theta} \ell(\Theta), \tag{11}$$

where $\Theta_1 = \log s_f, \Theta_{k+1} = \log \ell_k$. The initial value $\Theta_0 = \{\Theta_{1,0}, .., \Theta_{k+1,0}\}$ is used to start the optimization, where $\Theta_{1,0} = 0$ for the signal parameter and
$\Theta_{k+1,0} = \log(\frac{1}{3}L_k)$, for the length scale parameters with $L_k = b_k - a_k$. Knowing the hyper-parameters Θ^*, we can calculate the predictive statistics of outputs such as mean, error bar, and the probability distribution(PDF) at any test point $\mathbf{x}$. The predictive statistics of order q are obtained by considering that the power q of the response is also a MGPs conditional by the hyperparameters Θ^q. Let us write the predictive distribution for the q power of the response at $\mathbf{x}$ as predictive mean:

$$\mu_{\mathbf{f_r^q}}(\mathbf{x}; \Theta^q) = \sigma^q{}_{obs,r} \mathbf{c}^{q,T} (\mathbf{C}^q)^{-1} \mathbf{z_r} + \mu^q{}_{obs,\mathbf{r}}, \tag{12}$$

and predictive error bar:

$$\sigma^2_{\mathbf{f}^q_{\mathbf{r}}}(\mathbf{x};\Theta^q) = \sigma^2_{obs,\mathbf{r}}(\mathbf{c}(\mathbf{x},\mathbf{x};\Theta^q) - \mathbf{c}^{q,T}(\mathbf{C}^q)^{-1}\mathbf{c}^q), \tag{13}$$

where $\mathbf{c}^q = (\mathbf{C}(\mathbf{x},\mathbf{x}_1;\Theta^q),..,\mathbf{C}(\mathbf{x},\mathbf{x}_N;\Theta^q))$, $\mathbf{c}^{q,T}$ the transpose of $\mathbf{c}^q$, $(\mathbf{C}^q)^{-1}$ the inverse of the covariance $\mathbf{C}^q$, ${\sigma^q}_{obs,r}$, and ${\mu^q}_{obs,\mathbf{r}}$ are defined as in (Eq 7) and (Eq 8) using the q power of the observed response.
Integrating the (Eq 12) - (Eq 13) over the test point **x** we obtain the predictive mean and error bar of each moment, as: The predictive distribution:

$$m^q_r|D,\theta^q \sim N(\mu_{m^q_r};\sigma^2_{m^q_r}), \tag{14}$$

predictive mean:

$$\mu_{m^q_r} = \int_{\mathbf{X}} \mu_{\mathbf{f}^q_{\mathbf{r}}}(\mathbf{x};\Theta^q)p(\mathbf{x})d\mathbf{x}, \tag{15}$$

predictive error bar:

$$\sigma^2_{m^q_r} = \int_{\mathbf{X}} \sigma^2_{\mathbf{f}^q_{\mathbf{r}}}(\mathbf{x};\Theta^q)p(\mathbf{x})d\mathbf{x}. \tag{16}$$

The integration can be calculated using the Monte Carlo method.

We construct the nonstationary MGPs using several locally stationary MGPs obtained in the disjoint input space. The disjoint input space is obtained by dividing adaptively the input space into I disjoint subspace X^i, for $i = 1,..,I$, such that $X = \bigcup_{i=1}^{I} X^i$. The statistics of the whole domain ,called, global statistics are obtained by the combination of the statistics obtained over each child element X^i, $i = 1,..,I$. For each child element X^i, we have obtained a predictive distribution $m^{q,i}_r|D,\theta^q$ for (Eq 14) and the predictive mean $\mu_{m^{q,i}_r}$ and variance $\sigma^2_{m^{q,i}_r}$ using (Eq 15) and (Eq 16). The global statistics are obtained by the combination of all local statistics.

4. Numerical Results

Here we study a challenging problem in which the fracture propagates vertically within a three-layered medium, as described schematically in Figure 1. In this complex geological formation, the fracture growth tends to experiment a non-symmetric evolution growth due to abrupt changes in the confining stresses which assume different values at each layer (Σ^1_0 for the layer 1, Σ^2_0 layer 2 and Σ^3_0 for layer 3). The layers are separated by interfaces χ_1 and χ_2, that the fracture will pass through at unknown injection times. In such a scenario, numerical simulations of the fracture propagation might help the operation in the field, trying to reduce the risks or improving the stimulation. However, on accurate descriptions of the input parameters obtained by indirect measurements Ask (2003) might hamper the ability of the numerical model to deliver trustworthy predictions. So, in this work, we present a numerical modelling of HF which also take into account uncertainties inherited from imprecise measurement of rock properties by combining the robust numerical method developed in Peirce and Detourney (2008) , that takes care of the deterministic aspects of the problem, with the MGPs described before. Those uncertainties are represented in the model by considering some of the input parameters as random variables. We elected the Elasticity Modulus and the confining stresses on each layer as those uncertain parameters. Indeed, those choices entail a reasonable first scenario to be analyzed, as those parameters have an important impact on the fracturing, and their values in the technical literature show a substantial dispersion that could be represented with the help of a probabilistic model. The random Elasticity Modulus is considered homogenous along the medium and described as $G_E = E[G_E](1+\sigma_{G_E}\varepsilon_{G_E})$, where $E[G_E]$ is the expected value (mean) and σ_{G_E} the standard deviation. Moreover, ε_{G_E} is a uniform random variable with zero mean and unity variance. Each layer features its own random confining stress $\Sigma^i_0 = E[\Sigma^i_0](1+\sigma_{\Sigma^i_0}\xi_i)$ $(i = 1,..,3)$ where $E[\Sigma^i_0]$ and $\sigma_{\Sigma^i_0}$ represent, respectively, the mean and standard deviation, and ξ_i are independent uniform random variables with zero mean and unity variance. We are using simple stochastic models for the input parameters and will not discuss the sensitivity of the final results with regard to them, but in Zio and Rochinha (2012) we present a study assessing the impact of using different models, for the same raw data, in the predictions drawn from simulations.

The fracture takes place in a rocky medium consisting of three layers located at distances 918 m for layer 1, 928 m for layer 2 and 938 m for layer 3. The fracture is initiated in layer 2 and spreads in the layer 2 and 3. Taking in consideration typical values observed in this type of rock formation Mark D.Zoback (APRIL 10, 1992) and with a volumetric injection rate $Q_0 = 0.11m^2/s$. We obtain the dimensionless value of confining stress $\Sigma^1_0 = 1.25 \pm 0.02$, $\Sigma^2_0 = 1.41 \pm 0.041$, $\Sigma^3_0 = 1.45 \pm 0.031$. In the probabilistic model we consider that Σ^1_0, Σ^2_0, Σ^3_0 have a uniform distribution with mean $E[\Sigma^1_0]$=1.25, $E[\Sigma^2_0]$=1.41, $E[\Sigma^3_0]$=1.45 and the standard deviation $\sigma_{\Sigma^1_0}$=0.02, $\sigma_{\Sigma^2_0}$=0.041, $\sigma_{\Sigma^3_0}$=0.031. The Elasticity Modulus represented by G_E has as probabilistic model $G_E = E[G_E](1+\sigma_{G_E}\varepsilon_E)$, which has a uniform distribution with the mean $E[G_E]$ and the standard deviation σ_{G_E} which take values: $E[G_E] = 1$ and σ_{G_E}=0.15. The quantities of interest directly computed from the simulation are: fracture length on upper and lower $\ell_{up}(\tau,\varpi)$, $\ell_{low}(\tau,\varpi)$, the fracture aperture $\Omega(\chi, \tau, \varpi)$ and the fluid pressure $\Pi(\chi, \tau, \varpi)$. The HF process begins at the initial time $\tau_0 = 11.72$ and stops at time $\tau_f = 240$. The interfaces are located at the position $\chi_1 = 4.2$ and $\chi_2 = -7.5$ with respect to the well position $\chi = 0$ Figure 1. Analysing the deterministic solver using the expected value as nominal parameters, we observe that the fracture reaches the interface 1 and 2 at the respective time $\tau_{p1} \simeq 128$ and $\tau_{p2} \simeq 220$, as shown in Figure 2, which also presents the fracture aperture evolution at the interfaces. In Figure **??**, we present the fracture length on both sides. We observe that the evolution of the length in the upper and lower is the same until the HF fracture propagation reaches the first interface. When the fracture reaches the interface 2, the length of the fracture in the lower feels this effect and changes value abruptly. The contrast of confining stress can be seen in Figure 3 when the fracture propagation meets interface 2, the fracture aperture changes abruptly.

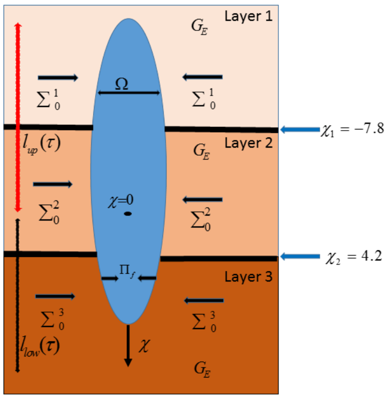

Figure 1. Schematic view of the layered medium

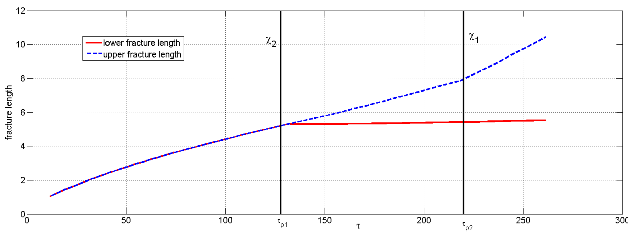

Figure 2. Fracture lengths at upper and lower $\ell_{up}(\tau)$ and $\ell_{low}(\tau)$

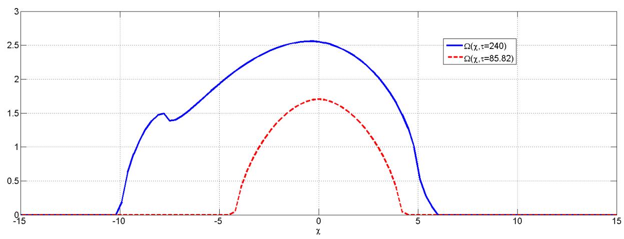

Figure 3. Fracture aperture at time $\tau = 240$

5. Computational performance

In order to assess the convergence of the MGPs method, we employ a reference solution obtained by the Monte Carlo (MC) method. This reference solution is obtained by analysing the convergence of some relevant outputs such as the final length of the fracture at lower and upper depicted at Figure 4. In these figures, we observed that 30,000 samples were enough to achieve an accurate approximation with the Monte Carlo method for the mean and variance of the outputs. Then we verify the efficiency of the new method called MGPs compared to the Stochastic Collocation method (SCM) and the Adaptive Stochastic Collocation method (ASCM) using the statistical solution of the Monte Carlo method obtained at 30,000 samples as reference solution. Therefore, we calculate the absolute error of the statistics such as the means and standard deviations of HF outputs which are a function of injection time τ. In this case, we construct the

MGPs by choosing as outputs, the lower length of the fracture $\ell_{low}(\tau)$ and the upper length $\ell_{up}(\tau)$ both with the total of 82 outputs, where $\tau = 82 : d\tau : 240$, with $d\tau = 3.9$. We construct the MGPs with different degree of prediction $\delta = 10^{-5}, 10^{-6}, 10^{-7}$. To obtain these degrees of predictions, the deterministic solver is respectively called at Nt=146, 755, and 3561 samples. For the same outputs, we calculate the statistics by using the SCM and the ASCM. The SCM statistics are obtained with the level 7 correspond to Nt=7537 and the statistics of the ASCM are obtained with $\delta = 10^{-6}$ correspond to Nt=10,073. Using the MGPs, the statistics are obtained by sampling the surrogate. Therefore, we need to know the ideal number of sampling Ns that can be used for sampling the surrogate. In Figures **??** - **??**, we present the absolute error of the mean $(mean_{err})$ and standard deviation (std_{err}) of outputs $\ell_{low}(\tau = 240)$ and $\ell_{up}(\tau = 240)$ obtained using different values of Ns. The absolute error is obtained by calculating the difference between the statistics obtained at Ns=20,000 and Ns<= $20,000$. We observe that the absolute error $(mean_{err})$ and (std_{err}) of both outputs begin converging at Ns=16,000 samples. However, we calculate the statistics by sampling the surrogate at Ns=20,000. In Figures 5 -6 we observe that the MGPs uses the few calls of deterministic solver to obtain the absolute error smaller than the SCM and ASCM absolute error i.e the MGPs solution is closed to the MC 30,000 with the fewest calls of the deterministic solver. These results show that the MGPs surrogate is efficient to calculate the statistical response of HF using few calls of the forward model.

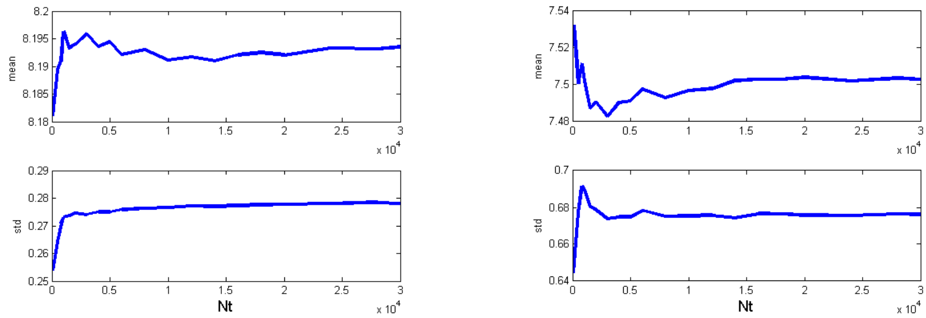

Figure 4. Convergence in mean and standard deviation of the fracture lower and upper length ℓ_{low} and ℓ_{up} at $\tau = 240$ using MC

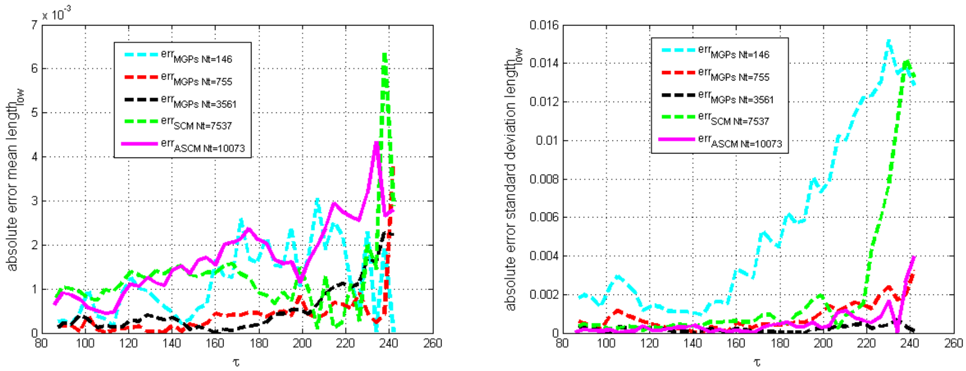

Figure 5. Evolution of the absolute error calculate using the mean and standard deviation of $\ell_{low}(\tau)$ obtained by the sampling of MGPs and the standard deviation of reference solution obtained by using MC at Nt=30,000

5.1 Nonstationary covariance function

The nonstationary MGPs is obtained by dividing adaptively the input space in disjoint subspace and in each subspace we use different covariance function to construct the local surrogate. The covariance function is conditioned by its hyperparameters represented by the signal strength $\mathbf{s_f} > 0$ and the length scale of each stochastic input $\{\ell_k\}_{k=1}^{K}$, where K the stochastic dimension is represented here by 4 input parameters such as the G_E, and the 3 confining stresses (Σ_0^1, Σ_0^2, Σ_0^3). The nonstationary MGPs can be seen by looking for the hyperparameters value obtained at each subregion. Taking as reference Figure 3, in which we present the evolution of the fracture aperture at the times $\tau = 85.82$ and $\tau = 240$. This figure show that the fracture aperture at time $\tau = 85.82$ has a smooth behavior because at this time, the HF did not reach any interfaces, whereas at the time $\tau = 240$ we observe the abrupt change of the aperture i.e the fracture aperture at this time has a non-smooth behavior. We construct two surrogates using respectively the fracture aperture at time $\tau = 85.82$ $\{\Omega(\chi, \tau = 85.82)\}$ and the aperture at the time $\tau = 240$ $\{\Omega(\chi, \tau = 240)\}$. The space in

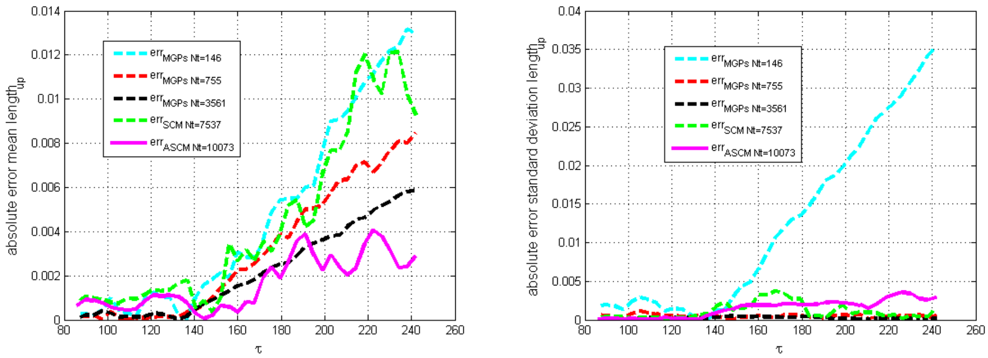

Figure 6. Evolution of the absolute error calculate using the mean and standard deviation of $\ell_{up}(\tau)$ obtained by the sampling of MGPs and the standard deviation of reference solution obtained by using MC at Nt=30,000

which the fracture will take place is discretized at 101 grid points, therefore, both surrogates are constructed respectively with the total of M=101 outputs. The surrogates are constructed with the same degree of prediction $\delta = 10^{-6}$. The surrogate with the outputs $\Omega(\chi, \tau = 85.82)$ is constructed after 2 divisions of the stochastic space i.e 2 subregions and the surrogate with the outputs $\Omega(\chi, \tau = 240)$ is constructed after 62 divisions of the stochastic space i.e 62 subregions. In Figure 7 we observe that the hyperparameters used to construct the covariance structure of the surrogate $\Omega(\chi, \tau = 85.82)$ are equal. This explains that a stationary covariance is used to approximate the smooth output $\Omega(\chi, \tau = 85.82)$. The outputs $\Omega(\chi, \tau = 240)$ is approximate using 61 local surrogates, in Figure 8, we present only the hyperparameters of the first 25 local surrogates, this is enough to observe that the nonstationary covariance structure is used to approximate the nonsmooth outputs $\Omega(\chi, \tau = 240)$. These results show that the MGPs constructs the adaptive covariance structure depending on the behavior, smooth/or non-smooth of the outputs.

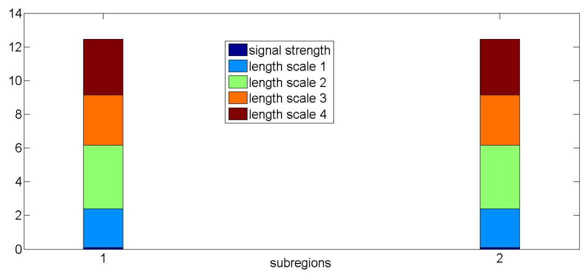

Figure 7. Hyperparameters of the surrogate $\Omega(\chi, \tau = 85.82)$ at each subregions

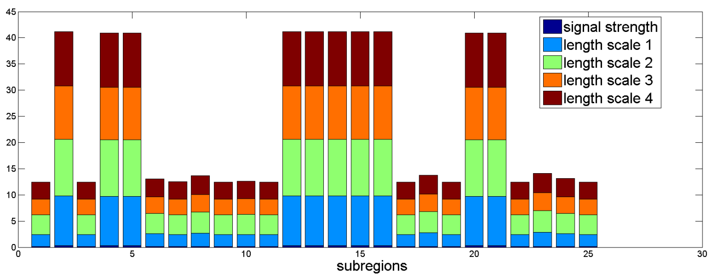

Figure 8. Hyperparameters of the surrogate $\Omega(\chi, \tau = 240)$ at each subregions

6. Conclusion

In this work, the we show the efficiency of MGPs to calculate with low computer cost the statistics of the HF in the complex rocky medium with the presence of a discontinuity. In the future work, we will use the MGPs to the application such as Uncertainty Quantification, Global sensitivity Analysis, and the Optimization under Uncertainty in the HF design.

7. REFERENCES

Ask, D., 2003. "Evaluation of measurement-related uncertainties in the analysis of overcoring rock stress from aspo hrl sweden a case study". *Rock Mech Mining Sci 40:1173-1187*.

George Shu Heng Pau, Y.Z., 9 May 2013. "Reduced order models for many-query subsurface flow applications". *Computational Geosciences, DOI 10.1007/s10596-013-9349-z*.

Gibbs, M., 1997. "Bayesian gaussian processes for classification and regression. phd thesis". *Univ.of Cambridge, Cambridge, U.K*.

Ilias Bilionis, Nicholas Zabaras, B.A.K., 2013. "Multi-output separable gaussian process: Towards an efficient, fully bayesian paradigm for uncertainty quantification". *Journal of Computational Physics*.

Ma, X. and Zabaras, N., 2008. "An adaptive hierarchical sparse grid collocation algorithm for the solution of stochastic differential equations". *Journal of Compuational Physics*.

Mark D.Zoback, J.H.H., APRIL 10, 1992. "In situ stress measurements to 3.5 km depth in the cajon pass scientific research borehole implications for the mechanics of crustal faulting". *JOURNAL OF GEOPHYSICAL RESEARCH, VOL. 97, NO. B4, PAGES 5039-5057*.

Peirce, Received 2 May 2014 accepted 22 August 2014 Available online 28 September 2014. "Modeling multi-scale processes in hydraulic fracture propagation using the implicit level set algorithm". *Department of Mathematics, University of British Columbia, Vancouver British Columbia V6T 1Z2 Canada*.

Peirce, A. and Detourney, E., 2008. "An implicit level set method for modeling hydraulically driven fractures". *Computer Methods in Applied Mechanics and Engineering 197, 2858-2885*.

S. Conti, A.O., 1992. "Bayesian statistics: Some bayesian numerical analysis". *Oxfort University Press*, Vol. 4, pp. 345–363.

Stefano Conti, A.O., 2010. "Bayesian emulation of complex multi-output and dynamic computer models". *Journal of Statistical Planning and Inference*.

Zio, S. and Rochinha, F.A., 2012. "A stochastic collocation approach for uncertainty quantification in hydraulic fracture numerical simulation". *International Journal for Uncertainty Quantification*, pp. 145–160.